

Behavior of the dielectric constant of Ar near the critical point

Marcelo Hidalgo, Kaline Coutinho, and Sylvio Canuto*

Instituto de Física, Universidade de São Paulo, Caixa Postal 66318, 05314-970, São Paulo, SP, Brazil

(Received 4 November 2014; published 11 March 2015)

The fundamental question of the behavior of the dielectric constant near the critical point is addressed using Ar as the probe system. The neighborhood of the liquid-vapor critical point of Ar is accessed by classical Monte Carlo simulation and then explicit quantum mechanics calculations are performed to study the behavior of the dielectric constant. The theoretical critical temperature is determined by calculating the position of the discontinuity of the specific heat and is found to be at $T_c^{\text{Theor}} = 148.7$ K, only 2 K below the experimental value. The large fluctuations and the inhomogeneity of the density that characterize the critical point rapidly disappear and are not seen at $T = T_c^{\text{Theor}} + 2$ K. The structure of Ar obtained by the radial distribution function is found to be in very good agreement with experiment both in the liquid phase and 2 K above the critical temperature. The behavior of the dielectric constant is then analyzed after calculating the static dipole polarizability and using a many-body Clausius-Mossotti equation. The dielectric constant shows a density-independent behavior around the critical density, 2 K above the critical temperature. At this point, the calculated value of the dielectric constant is 1.173 ± 0.005 in excellent agreement with the experimental value of 1.179.

DOI: [10.1103/PhysRevE.91.032115](https://doi.org/10.1103/PhysRevE.91.032115)

PACS number(s): 64.60.fh, 31.15.ap, 65.20.De

I. INTRODUCTION

The critical point of a fluid is located in the phase diagram at the end of the coexistence line between the gas and the liquid phases. As such it is the convergence point of the increasing density of the gas and the decreasing density of the liquid and is characterized by large fluctuations and density inhomogeneity. This point is the subject of intense experimental and theoretical interests, with emphasis on the behavior of the important thermodynamic functions. Some properties, such as the specific heat, are known to present singular behavior [1] near the critical point and to be characterized by universal critical exponents [2]. The behavior of the dielectric constant at the critical point of a fluid is less certain and has been a subject of great interest for many years where much still remains to be clarified. In previous studies Stell and Høye [3] have theoretically found that the dielectric constant of nonpolar fluids should remain finite at the critical point but exhibit singularities as a function of temperature. Several theoretical and experimental studies were made aiming at clarifying the existence and nature of the possible singularity [4–7]. Naturally, there is also interest in the density dependence of the dielectric constant and its behavior near the critical point. The behavior of the dielectric constant at the critical point is a fundamental problem with some pending answers. The subject is controversial and a singularity has not been detected in some specific experimental investigations [7]. Theoretical studies of the critical behavior of fluids have been conducted mostly by universal scaling functions [8–10] and renormalization theories [9, 11].

It is conceivable that looking at the problem with different techniques may clarify otherwise difficult points from the conventional perspective. With this in mind we adopt one alternative procedure that could allow a more close view with a microscopic quantum mechanical consideration. In this work we analyze the static dielectric constant of Ar slightly above the critical point by looking explicitly at the electronic structure of

the system. We use a multiscale approach combining classical simulation and quantum mechanics. Classical Monte Carlo (MC) simulations are performed to generate the configurations (position of the atoms) of the fluid at a given thermodynamic condition and quantum mechanical (QM) calculations are performed subsequently to obtain the electronic structure properties. Thus the QM calculations are made on configurations that are associated to a given thermodynamic condition. This procedure follows the successful multiscale approach that combines classical and quantum mechanical methods, originally devised by Levitt and Warshel [12] for treating enzymatic chemical reactions. It can be extended for the study of liquid and fluid systems [13] with thermodynamic condition imposed by the classical simulation and subsequent quantum mechanical calculations giving the electronic structure. This present work gives explicitly calculated values of the dielectric constant in the close vicinity of the critical point ($T > T_c$). Thus, the behavior of the dielectric constant, only slightly above the critical point, is determined using first-principle quantum mechanical calculations.

II. METHODS AND RESULTS

We use a sequential QM-MC approach [13], first generating the atomic configurations of the fluid and performing QM calculations using these configurations. The Metropolis MC simulations are performed in the NVT ensemble, which is more convenient for the analysis of the results as a function of the density. In some specific cases the NPT ensemble will also be used. We adopt the standard procedures [14], such as the image method combined with the periodic boundary conditions of a cubic box of size L , the cutoff radius ($r_c = L/2$) and the long range correction of the energy beyond the r_c assuming a uniform radial distribution [$G(r) \approx 1$]. The Ar atoms interact via the conventional Lennard-Jones potential with the parameters devised by Maitland and Smith [15] ($\epsilon = 0.2378$ kcal/mol and $\sigma = 3.41$ Å). As we will see, this potential gives an accurate description of the configuration

*Corresponding author: canuto@if.usp.br

of Ar fluid in the vicinities of the critical point. All MC simulations were performed with the DICE program [16].

As we will approach the critical point it is important to determine its location in the phase diagram of Ar associated with this classical potential. Instead of the conventional and laborious procedure of calculating isotherms in the P - V diagram we will look for the specific heat c_v . This was obtained after the MC simulation using the expression [14]

$$\langle c_v \rangle = \frac{3}{2}k_B T + \frac{(\langle U^2 \rangle - \langle U \rangle^2)}{Nk_B T}, \quad (1)$$

where the first term comes from the equipartition theorem, the second term comes from the fluctuation of the potential energy U , and k_B is the Boltzmann constant. We note that the potential of Maitland and Smith [15] adopted here reproduces well the value of the specific heat c_v for various thermodynamic conditions. For instance, for $T = 120$ K and density 1.166 g/cm³ we calculate the value of c_v as 4.32 ± 0.12 cal/mol K in very good comparison with the experimental [17] result of 4.30 cal/mol K. Hence we will attempt to determine the critical temperature by looking at the singularity of the specific heat. In Fig. 1 we then show the calculated specific heat c_v , using Eq. (1), along the isochoric $\rho_c = 0.531$ g/cm³. The divergence of the critical point cannot be seen with a reduced number of particles. With 1500 Ar atoms there appears the indication of the critical point but the divergence is clear only for a large number of particles. Using 2500 Ar atoms the calculated value of c_v at 148.7 K is $\sim 10^5$ kcal/mol K. This very large value is outside the scale of Fig. 1 and the dashed line is intended to guide the eye. Therefore, it is possible to discern the divergence of c_v characterizing the theoretical critical temperature, $T_c^{\text{Theor}} = 148.7$ K. This critical temperature is 2 K below the experimental value of 150.7 K. The large fluctuations at the critical point are known to rapidly disappear as we increase the temperature. Thus to avoid the large fluctuations and density inhomogeneity of the critical point

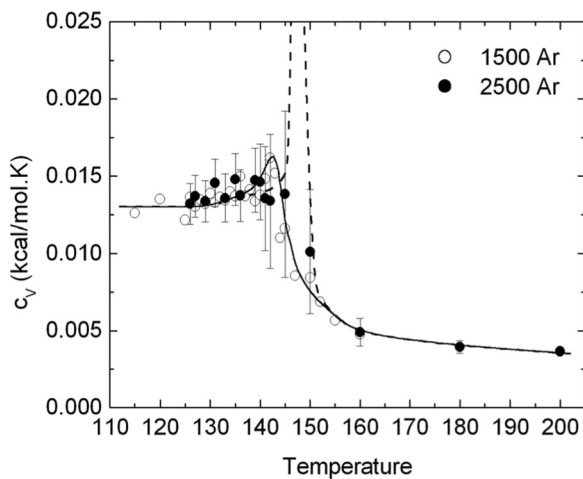


FIG. 1. The calculated specific heat c_v of Ar along the critical isochoric $\rho_c = 0.531$ g/cm³. The calculated value of c_v at 148.7 K is $\sim 10^5$ kcal/mol K. This very large value is outside the scale. The lines are drawn only to guide the eye through the points for 1500 Ar (solid) and 2500 Ar (dashed). For simplicity the standard deviations are presented only for the 2500 Ar simulations.

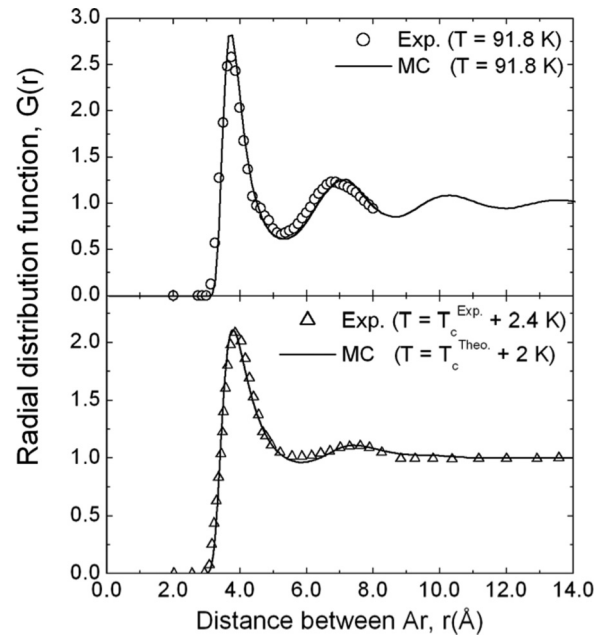


FIG. 2. The calculated radial distribution functions of Ar at the liquid phase (top) and 2 K above the critical point (bottom) and comparison with experimental results [20].

and at the same time remain in the close vicinity we analyze the dielectric constant of Ar at $T = T_c^{\text{Theor}} + 2$ K.

In every case, after equilibration, 12.5×10^6 MC steps are performed to obtain the atomic arrangements at given thermodynamic conditions. The configurations are then sampled for the subsequent QM calculations. For every thermodynamic condition adopted, 150 configurations are extracted from the MC simulation with less than 10% of statistical correlation. These are separated for the subsequent QM calculations. The statistical correlation is obtained calculating the autocorrelation function of the energy [18,19]. The QM calculations are made using the first coordination that is composed of one central reference Ar surrounded by an additional 13 Ar atoms. This corresponds to the first solvation shell at the liquid condition of $T = 91.8$ K and $P = 1.8$ atm. For consistency, we use this number of atoms even in the low-density regime. For instance, near the critical point ($T_c^{\text{Theor}} + 2$ K and $\rho_c = 0.531$ g/cm³) this corresponds to including all atoms around a central Ar, within a distance of 7.3 Å, thus extending beyond the first solvation shell that is seen to end at 5.8 Å (Fig. 2) with a broad but clear solvation shell. Figure 2 shows the calculated radial distribution function for the liquid condition ($T = 91.8$ K) and also near the critical point ($T = T_c^{\text{Theor}} + 2$ K) and compares these with the experimental results obtained from x-ray diffractions [20]. The experimental studies of Mikolaj and Pings [20] have considered T also slightly above the critical point at about 153.1 K ($T = T_c^{\text{Expt}} + 2.4$ K) and the critical density of $\rho = 0.531$ g/cm³ and this is the result shown in Fig. 2 for comparison. The agreement is seen to be excellent, corroborating the MC simulation and its accuracy in generating the configurations of the fluid both in the liquid phase and close to the critical point. In addition Fig. 2 also shows that the structure of Ar only 2 K above the critical temperature is well defined and the agreement between theory and experiment

is excellent. At this temperature the structure is indeed well described and statistically converged results will be obtained for the calculated dielectric constant.

For nonpolar gaseous systems the Clausius-Mossotti (CM) equation relates the static (frequency-independent) dipole polarizability to the static dielectric constant. The validity and accuracy of the CM equation for imperfect gases, liquids, and dense systems has been analyzed on different occasions, since the early days [21]. Experimentally, Amey and Cole [22] systematically noted that the difference in the CM equation between liquid and gaseous Ar is mild and it could be associated with the effective polarizability produced by the interaction with the neighbor atoms. The overlap of the electron densities, in particular, should be considered when treating liquid systems. This is expected because the increased density of the liquid imposes the need for explicit consideration of the atomic interaction. Zwanzig and co-workers [23] have analyzed analytically the correction to the related Lorentz-Lorenz equation at the critical point of Ar and concluded that it is very small.

In this work atom-atom interaction will be included naturally by considering the Schrödinger equation for the system, composed by 14 Ar atoms. The wave function is determined for the entire system in each configuration sampled in every thermodynamic condition, being antisymmetric with respect to the interchange of electrons of all Ar atoms. This allows the wave function to delocalize over the system including also overlap and exchange interaction between the different Ar atoms. Hence, our procedure calculates the density-dependent dipole polarizability of the Ar atom in the specific thermodynamic condition and the dielectric constant is obtained from the all-electron CM equation. Analyzing the density dependence of the dielectric constant we may corroborate the experimental evidences and theoretical expectations. For each configuration i that is sampled from the MC simulation ($i = 1, 150$) the dipole polarizability α_i of the central Ar atom in the explicit presence of the 13 nearest neighbors is determined. For each α_i obtained by QM calculation, we calculate the corresponding dielectric constant ε_i by using the CM equation:

$$\frac{\varepsilon_i - 1}{\varepsilon_i + 2} = \frac{4\pi}{3} \alpha_i \rho \frac{N_A}{M} \quad i = 1150, \quad (2)$$

where ρ is the density, N_A is the Avogadro number, and M is the molar mass. Hence, the distribution of values for the dielectric constant, $\{\varepsilon_i\}$, in a specific thermodynamic condition is calculated and from this distribution we obtain also the average value of $\langle \varepsilon \rangle$ and the standard deviation, σ . Therefore, all the values described by $\langle \varepsilon \rangle \pm \sigma$ have the 68%

of confidence determined by Gaussian distributions. Different thermodynamic conditions are used and in every one a total of 150 configurations composed of one central and an additional 13 Ar atoms are used to obtain the statistically converged average dielectric constant. Considering all thermodynamic conditions of this work, more than 3000 QM calculations were performed. The QM density-functional calculations are performed using the Kohn-Sham approach [24]. We have used the Becke [25] three-parameter functional with the exchange correlation due to Perdew [26], combined with the aug-cc-pVDZ basis set [27], B3P86/aug-cc-pVDZ. At some specific points we have also used the dispersion-corrected wB97-D functional [28] with the same basis set. But the calculated dipole polarizabilities differ by less than $0.04 a_0^3$, equivalent to the standard deviation. All QM calculations were made using the GAUSSIAN-09 program [29].

The selection of the QM level adopted is based on the calculated values of the dielectric constant of isolated (i.e., noninteracting system corresponding to the very low density of the gas phase) Ar and also in the liquid phase. For instance, at $T = 91.8$ K and $P = 1.8$ atm we obtain a calculated density of 1.362 ± 0.015 g/cm³ compared to the experimental value [20] of 1.365 g/cm³. The corresponding average dielectric constant is 1.519, in close agreement with the experimental value [30] of 1.521, obtained at $T = 87.4$ K and $P = 1.0$ atm. This gives great credence to the present model and the approximations involved.

Before considering the critical point we discuss the results of the calculated values of the dielectric constant in the isothermal situation with varying values of pressure. In such cases the MC simulations are made using the NPT ensemble. Table I shows the different values of pressure used for a constant temperature of 91.8 K. We see in this table that increasing the pressure by a factor of nearly 20, only small changes in the calculated density and in the static polarizability are obtained. Hence, the dielectric constant is seen to be insensitive to great variations of pressure when in the liquid phase. For an indication of the reliability of these calculated results we compare with experiment. For instance, at 1.8 atm, the theoretical results for the density and dielectric constants are 1.362 g/cm³ and 1.519. These results are in excellent agreement with the corresponding experimental values [20,30] of 1.365 g/cm³ and 1.521, respectively.

Now we consider the thermodynamic condition 2 K above T_c^{Theor} and density $\rho_c = 0.531$ g/cm³. QM calculations are made to obtain the static dipole polarizability α_i for each of the 150 configurations. The statistically converged average value at this point is then obtained as $\alpha = 10.878 \pm 0.030 a_0^3$.

TABLE I. Calculated values for the density, static dipole polarizability, and dielectric constant for temperature $T = 91.8$ K and different pressures. Standard deviations are 0.015 g/cm³, 0.030 a_0^3 , and 0.005 for the density, polarizability, and dielectric constants, respectively.

Pressure, P (atm)	Density, ρ (g/cm ³)	Polarizability, $\alpha(a_0^3)$	Dielectric constant, ε
1.8 ^a	1.362	11.529	1.519
17	1.368	11.544	1.523
22	1.368	11.544	1.523
27	1.370	11.548	1.524
32	1.372	11.543	1.520

^aWith pressure of 1.8 atm the experimental value of the density [20] is 1.365 g/cm³ and the dielectric constant [30] is 1.521.

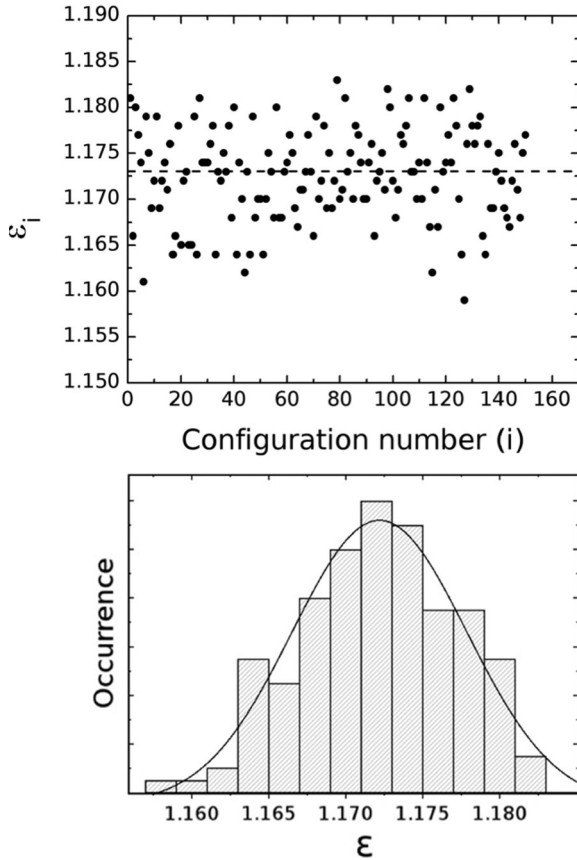


FIG. 3. Statistical distribution of values calculated for the dielectric constant. Top shows the specific values and bottom shows the corresponding histogram and Gaussian distribution with average value of 1.173 and the standard deviation of 0.005.

For each value of the polarizability α_i a corresponding dielectric constant ϵ_i is obtained using Eq. (2). Figure 3 shows the distribution of these values with ϵ_i , ranging between a maximum and a minimum, within 1.185 and 1.155. The calculated values follow a Gaussian distribution also shown in Fig. 3 (bottom), and with an average value $\epsilon = 1.173$ and standard deviation $\sigma = 0.005$. This is our theoretical value of the dielectric constant of Ar in the close vicinity of the critical point, only 2 K above it. Experimental results for the dielectric constant are somewhat difficult to obtain due to possible spurious effects such as temperature gradients [31]. For the case of Ar, the experimental value [32] has been carefully determined from the density dependence of the static (infinite wavelength) refractive index as 1.179, a value that is in excellent agreement with our result of 1.173 ± 0.005 .

III. DISCUSSIONS ON THE BEHAVIOR OF THE DIELECTRIC CONSTANT

After a successful description of the dipole polarizability and the dielectric constant at different thermodynamic conditions we now consider their behavior near the critical point at the one-phase region ($T > T_c$), thus avoiding the possibility of phase transition. Using the same procedure we have obtained the dielectric constant near the critical point. Figure 4 (top) shows the behavior of the dielectric constant as a function

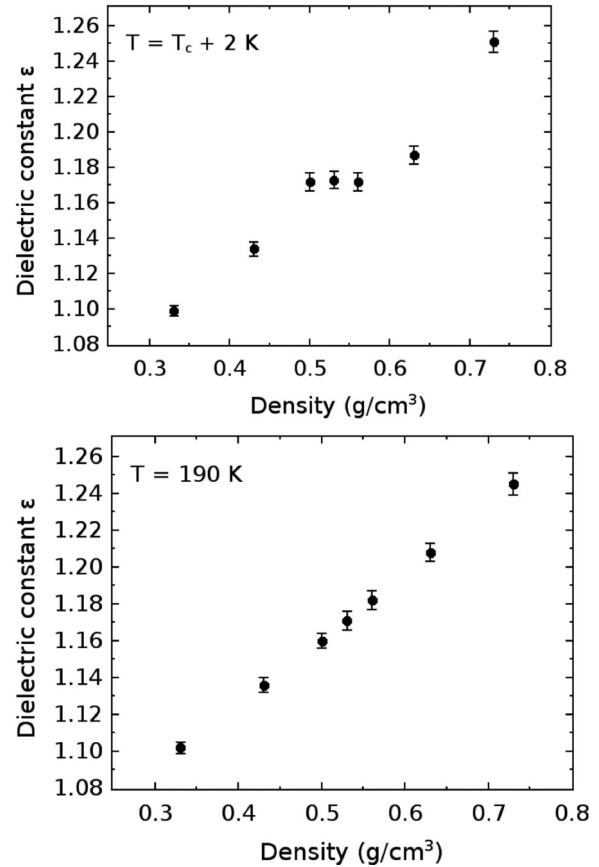


FIG. 4. Variation of the calculated dielectric constant of Ar with the density. The behavior is linear for $T = 190$ K but shows a different characteristic close to the critical point ($T = T_c^{\text{Theor}} + 2$ K and $\rho_c = 0.531$ g/cm³).

of the density. Each point in this diagram corresponds to an average value of the dielectric constant obtained from 150 QM calculations using configurations sampled from the MC simulation in the particular thermodynamic condition (NVT ensemble with fixed density and temperature). The results are also shown numerically in Table II, and it can be seen that there is a linear behavior of the dielectric constant with the density outside the region of close proximity to the critical

TABLE II. Calculated values for the static dipole polarizability and dielectric constant for temperature $T = T_c^{\text{Theor}} + 2$ K and different densities. Standard deviations are $0.030 a_0^3$ and 0.005 for the polarizability and dielectric constants, respectively. Experimental value [32] of the static dielectric constant at the critical point ($T_c = 150.7$ K and $\rho_c = 0.531$ g/cm³) is 1.179.

Density, ρ (g/cm ³)	Polarizability, $\alpha(a_0^3)$	Dielectric constant, ϵ
0.330	10.617	1.099
0.430	10.717	1.134
0.500	10.837	1.172
0.531	10.878	1.173
0.560	10.874	1.172
0.630	10.943	1.187
0.730	11.038	1.251

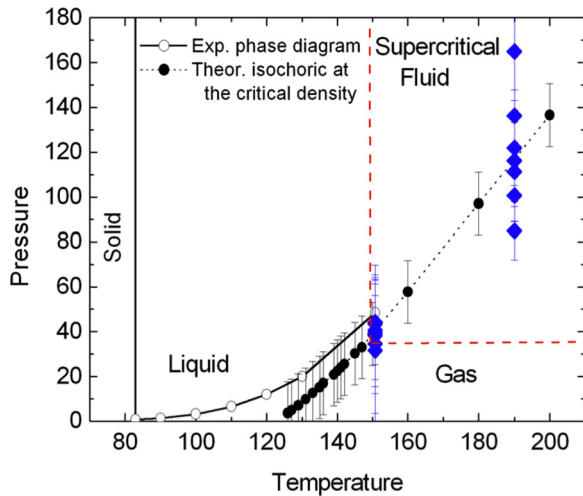


FIG. 5. (Color online) Phase diagram showing the calculated points corresponding to the varying densities of Fig. 4 along the two isotherms ($T = T_c^{\text{Theor}} + 2$ K and $T = 190$ K). Pressures are obtained directly from the NVT simulation. For $T = 190$ K all points are in the supercritical region.

point. For the low density $\rho = 0.33$ g/cm³ the calculated dielectric constant is 1.099 ± 0.005 whereas for the relatively high density $\rho = 0.73$ g/cm³ it is 1.251 ± 0.005 . However, as it can be seen around $\rho_c = 0.531$ g/cm³, within the theoretical accuracy, the dielectric constant becomes insensitive to small changes in the density. The calculated dielectric constants have the same value within the standard deviation. This is in clear contrast (Fig. 4, bottom) when considering the density dependence in the bulk of the supercritical region with $T = 190$ K. In this case the dielectric constant increases linearly for all values of the density within the range considered. This linear increase is in line with the linear increase of the average polarizability and hence in agreement with the experiments of Johnston *et al.* [22] that determined this linear increase of the Clausius-Mossotti function for Ar, N, and CH₄ at pressures below 100 atm. The present results (Fig. 4, top) show that the dielectric constant around the critical point has

a peculiar behavior exhibiting a regime where it is density independent. This is also in keeping with the experiments performed by Chan [7] for the Ne case where the dielectric constant was found to be insensitive to the density within the interval $|(\rho - \rho_c)/\rho_c| \leq 0.05$. In fact, Chan [7] has conducted a careful experimental investigation of the dielectric constant of Ne near its liquid-vapor critical point. Their measurements indicate that within the experimental accuracy the dielectric constant is density independent in the proximities of the critical point. Our approach with first-principle quantum mechanical calculations gives that slightly above the vapor-liquid critical temperature the dielectric constant around the critical isochoric becomes insensitive to small changes in the density, opposite to what is obtained aside this thermodynamic condition, where it increases linearly with the density. It can be seen in Fig. 4 (top) that there are two different inclinations for the linear increase before and after the critical point. This is an indication of the change of regime at the one-phase region ($T > T_c$) where the pressure variation along the isotherm ($T = T_c^{\text{Theor}} + 2$ K) indicates a change from the supercritical to the gas condition. The situation is clearly demonstrated in Fig. 5 where the two isotherms are shown in the calculated phase diagram, using the values calculated for the pressure in each case.

IV. SUMMARY AND CONCLUSIONS

We have addressed the fundamental question of the behavior of the static dielectric constant near the liquid-vapor critical point using Ar as the probe system. Our multiscale results obtained by combining statistical mechanics and first-principle quantum mechanics indicate that the dielectric constant of Ar only 2 K above T_c and around the critical isochoric becomes density independent, and our calculated value of 1.173 ± 0.005 is in excellent agreement with the experimental value of 1.179.

ACKNOWLEDGMENTS

We acknowledge discussions with Professor M. J. Oliveira and Professor S. Salinas. This work has been partially supported by CNPq, CAPES INCT-FCx, NAP-FCx, BioMol, and FAPESP (Brazil).

-
- [1] M. I. Bagatski, A. V. Voronel, and V. G. Gusak, *Sov. Phys. JETP-USSR* **16**, 517 (1963); M. E. Fisher, *Phys. Rev.* **136**, A1599 (1964).
 - [2] M. E. Fisher, in *Critical Phenomena*, Lecture Notes in Physics Vol. 186, edited by F. J. W. Hahne (Springer, Berlin, 1982), pp. 1–139.
 - [3] G. Stell and J. S. Høye, *Phys. Rev. Lett* **33**, 1268 (1974).
 - [4] J. V. Sengers, D. Bedeaux, P. Mazur, and S. C. Greer, *Physica* **104**, 573 (1980).
 - [5] G. Ascarello and H. Nakanishi, *J. Phys. (Paris)* **51**, 341 (1990).
 - [6] C. E. Bertrand, J. V. Sengers, and M. A. Anisimov, *J. Phys. Chem. B* **115**, 14000 (2011).
 - [7] M. H. W. Chan, *Phys. Rev. B* **21**, 1187 (1980).
 - [8] M. E. Fisher, *Rep. Prog. Phys.* **30**, 615 (1967).
 - [9] H. E. Stanley, *Rev. Mod. Phys.* **71**, S358 (1999).
 - [10] L. P. Kadanoff, in *The Oxford Handbook of Philosophy Physics*, edited by R. Batterman (Oxford University Press, Oxford, 2011).
 - [11] N. Goldenfeld, *Lectures on Phase Transitions and the Renormalization Group* (Addison-Wesley, Reading, MA, 1993).
 - [12] A. Warshel and M. Levitt, *J. Mol. Biol.* **103**, 227 (1976).
 - [13] K. Coutinho, S. Canuto, and M. C. Zerner, *Int. J. Quantum Chem.* **65**, 885 (1997); W. R. Rocha, K. Coutinho, W. B. de Almeida, and S. Canuto, *Chem. Phys. Lett.* **335**, 127 (2001); E. E. Fileti, K. Coutinho, T. Malaspina, and S. Canuto, *Phys. Rev. E* **67**, 061504 (2003); M. Hidalgo and S. Canuto, *Phys. Lett. A* **377**, 1720 (2013).
 - [14] M. P. Allen and D. J. Tildesley, *Computer Simulation of Liquids* (Clarendon Press, Oxford, 1987).

- [15] G. C. Maitland and E. B. Smith, *Mol. Phys.* **22**, 861 (1971).
- [16] K. Coutinho and S. Canuto, *DICE (version 2.9): A general Monte Carlo program for liquid simulation*, University of São Paulo, 2009.
- [17] *Simple Dense Fluids*, edited by H. L. Frisch and Z. W. Salsburg (Academic Press, New York, 1968).
- [18] K. Coutinho, M. J. Oliveira, and S. Canuto, *Int. J. Quantum Chem.* **66**, 249 (1998).
- [19] C. Chatfield, *The Analysis of Time Series. An Introduction*, 3rd ed. (Chapman and Hall, London, 1984).
- [20] A. Eisenstein and N. S. Gingrich, *Phys. Rev.* **62**, 261 (1942); P. G. Mikolaj and C. J. Pings, *J. Chem. Phys.* **46**, 1401 (1967).
- [21] J. G. Kirkwood, *J. Chem. Phys.* **4**, 592 (1936); H. H. Uhlig, J. G. Kirkwood, and F. G. Keyes, *ibid.* **1**, 155 (1933); L. Jansen and P. Mazur, *Physica* **21**, 193 (1955); L. Jansen, *Phys. Rev.* **112**, 434 (1958); R. W. Zwanzig, *J. Chem. Phys.* **25**, 211 (1956); **27**, 821 (1957); A. D. Buckingham and J. A. Pople, *Trans. Faraday Soc.* **51**, 1029 (1957).
- [22] D. R. Johnston, G. J. Ouderman, and R. H. Cole, *J. Chem. Phys.* **33**, 1310 (1960); R. L. Amey and R. H. Cole, *ibid.* **40**, 146 (1964).
- [23] S. Y. Larsen, R. D. Mountain, and R. Zwanzig, *J. Chem. Phys.* **42**, 2187 (1965).
- [24] W. Kohn and L. J. Sham, *Phys. Rev.* **140**, A1133 (1965).
- [25] A. D. Becke, *J. Chem. Phys.* **98**, 5648 (1993).
- [26] J. P. Perdew, *Phys. Rev. B* **33**, 8822 (1986).
- [27] D. E. Woon and T. H. Dunning, Jr., *J. Chem. Phys.* **98**, 1358 (1993).
- [28] J.-D. Chai and M. Head-Gordon, *Phys. Chem. Chem. Phys.* **10**, 6615 (2008).
- [29] M. J. Frisch *et al.*, *Gaussian 09, Revision A.1* (Gaussian, Inc., Wallingford, CT, 2009).
- [30] J. McLennan, R. Hoyt, and J. Wilhelm, *Trans. R. Soc. Can.* **24**, 37 (1930); see also *Handbook of Chemistry and Physics*, 73rd ed., edited by D. R. Lide (CRC Press, Boca Raton, FL, 1993), p. 9.51.
- [31] T. Doiron and H. Meyer, *Phys. Rev. B* **17**, 2141 (1978).
- [32] R. K. Teague and C. J. Pings, *J. Chem. Phys.* **48**, 4973 (1968).